

# Online Research @ Cardiff

This is an Open Access document downloaded from ORCA, Cardiff University's institutional repository: <https://orca.cardiff.ac.uk/130862/>

This is the author's version of a work that was submitted to / accepted for publication.

Citation for final published version:

Kaneko, Daisuke, Adachi, S., Ade, P. A. R., Aguilar Faúndez, M., Akiba, Y., Arnold, K., Baccigalupi, C., Barron, D., Beck, D., Beckman, S., Bianchini, F., Boettger, D., Borrill, J., Carron, J., Chapman, S., Cheung, K., Chinone, Y., Crowley, K., Cukierman, A., Dobbs, M., Dunner, R., El-Bouhargani, H., Elleflot, T., Errard, J., Fabbian, G., Feeney, S. M., Feng, C., Fujino, T., Galitzki, N., Gilbert, A., Goeckner-Wald, N., Groh, J., Hall, G., Halverson, N. W., Hamada, T., Hasegawa, M., Hazumi, M., Hill, C. A., Howe, L., Inoue, Y., Jaehnig, G., Jeong, O., Katayama, N., Keating, B., Keskitalo, R., Kikuchi, S., Kisner, T., Krachmalnicoff, N., Kusaka, A., Lee, A. T., Leon, D., Linder, E., Lowry, L. N., Mangu, A., Matsuda, F., Minami, Y., Navaroli, M., Nishino, H., Peloton, J., Pham, A. T. P., Poletti, D., Puglisi, G., Reichardt, C. L., Ross, C., Segawa, Y., Silva-Feaver, M., Siritanasak, P., Stebor, N., Stompor, R., Suzuki, A., Tajima, O., Takakura, S., Takatori, S., Tanabe, D., Teply, G. P., Tomaru, T., Tsai, C., Verges, C., Westbrook, B. and Zhou, Y. 2020. Deployment of POLARBEAR-2A. *Journal of Low Temperature Physics* 199 , pp. 1137-1147. 10.1007/s10909-020-02366-w file

Publishers page: <http://dx.doi.org/10.1007/s10909-020-02366-w>  
<<http://dx.doi.org/10.1007/s10909-020-02366-w>>

Please note:

Changes made as a result of publishing processes such as copy-editing, formatting and page numbers may not be reflected in this version. For the definitive version of this publication, please refer to the published source. You are advised to consult the publisher's version if you wish to cite this paper.

This version is being made available in accordance with publisher policies.

See

<http://orca.cf.ac.uk/policies.html> for usage policies. Copyright and moral rights for publications made available in ORCA are retained by the copyright holders.



[Click here to view linked References](#)

**Journal of Low Temperature Physics manuscript No.**  
(will be inserted by the editor)

## Deployment of POLARBEAR-2A

Daisuke Kaneko<sup>a</sup> · S. Adachi<sup>b</sup> · P. A. R. Ade<sup>c</sup> ·  
 M. Aguilar<sup>d</sup> · Y. Akiba<sup>e,f</sup> · K. Arnold<sup>g</sup> ·  
 C. Baccigalupi<sup>h,i</sup> · D. Barron<sup>j</sup> · D. Beck<sup>k</sup> ·  
 S. Beckman<sup>l</sup> · F. Bianchini<sup>m</sup> · D. Boettger<sup>n</sup> ·  
 J. Borrill<sup>o,p</sup> · J. Carron<sup>q</sup> · S. Chapman<sup>r</sup> ·  
 K. Cheung<sup>l</sup> · Y. Chinone<sup>a,l</sup> · K. Crowley<sup>g</sup> ·  
 A. Cukierman<sup>s</sup> · M. Dobbs<sup>t</sup> · R. Dunner<sup>n</sup> ·  
 H. El-Bouhargani<sup>k</sup> · T. Elleflot<sup>g</sup> · J. Errard<sup>k</sup> ·  
 G. Fabbian<sup>q</sup> · S. M. Feeney<sup>u</sup> · C. Feng<sup>v</sup> ·  
 T. Fujino<sup>w</sup> · N. Galitzki<sup>g</sup> · A. Gilbert<sup>t</sup> ·  
 N. Goeckner-Wald<sup>l</sup> · J. Groh<sup>l</sup> · G. Hall<sup>x</sup> ·  
 N. W. Halverson<sup>y,z</sup> · T. Hamada<sup>e,aa</sup> ·  
 M. Hasegawa<sup>e,f</sup> · M. Hazumi<sup>a,e,f,ab</sup> · C. A. Hill<sup>l,ac</sup> ·  
 L. Howe<sup>g</sup> · Y. Inoue<sup>ad</sup> · G. Jaehnig<sup>y,z</sup> · O. Jeong<sup>l</sup> ·  
 N. Katayama<sup>a</sup> · B. Keating<sup>g</sup> · R. Keskitalo<sup>o,p</sup> ·  
 S. Kikuchi<sup>w</sup> · T. Kisner<sup>o,p</sup> · N. Krachmalnicoff<sup>h</sup> ·  
 A. Kusaka<sup>a,ac,ae</sup> · A. T. Lee<sup>l,ac,af</sup> · D. Leon<sup>g</sup> ·  
 E. Linder<sup>o,ac</sup> · L. N. Lowry<sup>g</sup> · A. Mangu<sup>l,ac</sup> ·  
 F. Matsuda<sup>a</sup> · Y. Minami<sup>e</sup> · M. Navaroli<sup>g</sup> ·  
 H. Nishino<sup>ag</sup> · J. Peloton<sup>ah</sup> · A. T. P. Pham<sup>m</sup> ·  
 D. Poletti<sup>h</sup> · G. Puglisi<sup>ai</sup> · C. L. Reichardt<sup>m</sup> ·  
 C. Ross<sup>r</sup> · Y. Segawa<sup>e,f</sup> · M. Silva-Feaver<sup>g</sup> ·  
 P. Siritanasak<sup>g</sup> · N. Stebor<sup>aj</sup> · R. Stompor<sup>k</sup> ·  
 A. Suzuki<sup>ac</sup> · O. Tajima<sup>b</sup> · S. Takakura<sup>a</sup> ·  
 S. Takatori<sup>e,f</sup> · D. Tanabe<sup>e,f</sup> · G. P. Teplý<sup>g</sup> ·  
 T. Tomaru<sup>ak</sup> · C. Tsai<sup>g</sup> · C. Verges<sup>k</sup> ·  
 B. Westbrook<sup>af</sup> · Y. Zhou<sup>l</sup>

the date of receipt and acceptance should be inserted later

---

<sup>a</sup>Kavli Institute for the Physics and Mathematics of the Universe (WPI), UTIAS, the University of Tokyo, Kashiwa, Chiba 277-8583, Japan · <sup>b</sup>Department of Physics, Kyoto University · <sup>c</sup>School of Physics and Astronomy, Cardiff University · <sup>d</sup>Departamento de Física, FCFM, Universidad de Chile · <sup>e</sup>High Energy Accelerator Research Organization (KEK) · <sup>f</sup>The Graduate University for Advanced Studies (SOKENDAI) · <sup>g</sup>Department of Physics, University of California, San Diego · <sup>h</sup>The International School for Advanced Studies (SISSA) · <sup>i</sup>The National Institute for Nuclear Physics (INFN) · <sup>j</sup>Department of Physics and Astronomy, University of New Mexico · <sup>k</sup>AstroParticule et Cosmologie, Université Paris Diderot · <sup>l</sup>Department of Physics, University of California, Berkeley · <sup>m</sup>School of Physics, University of Melbourne · <sup>n</sup>Centro de Astro-Ingeniería, Pontificia Universidad Católica de Chile · <sup>o</sup>Space Sciences Laboratory, University of California · <sup>p</sup>Computational Cosmology Center, Lawrence Berkeley National Laboratory, <sup>q</sup>Department of Physics and Astronomy, University of Sussex · <sup>r</sup>Department of Physics and Atmospheric Science, Dalhousie University · <sup>s</sup>Kavli Institute for Particle Astrophysics and Cosmology, Stanford University · <sup>t</sup>Physics Department, McGill University · <sup>u</sup>Center for Computational Astrophysics, Flatiron Institute · <sup>v</sup>Department of Physics, University of Illinois at Urbana-Champaign · <sup>w</sup>College of Engineering Science, Yokohama National University · <sup>x</sup>School of Physics and Astronomy, University of Minnesota · <sup>y</sup>Center for Astrophysics and Space Astronomy, University of Colorado · <sup>z</sup>Department of Physics, University of Colorado · <sup>aa</sup>Astronomical Institute, Graduate School of Science, Tohoku University · <sup>ab</sup>Institute of Space and Astronautical Science, Japan Aerospace Exploration Agency · <sup>ac</sup>Physics Division, Lawrence Berkeley National Laboratory · <sup>ad</sup>Department of Physics, National Central University · <sup>ae</sup>Department of Physics, School of

1  
2  
3  
4  
5  
6  
7  
8  
9  
10  
11  
12  
13  
14  
15  
16  
17  
18  
19  
20  
21  
22  
23  
24  
25  
26  
27  
28  
29  
30  
31  
32  
33  
34  
35  
36  
37  
38  
39  
40  
41  
42  
43  
44  
45  
46  
47  
48  
49  
50  
51  
52  
53  
54  
55  
56  
57  
58  
59  
60  
61  
62  
63  
64  
65

**Abstract** POLARBEAR-2A is the first of three receivers in the Simons Array, a cosmic microwave background experiment located on the Atacama Plateau in Chile. POLARBEAR-2A was deployed and achieved the first light in January 2019 by mapping the microwave emission from planet observations. Commissioning work is underway to prepare the receiver for science observations.

**Keywords** CMB,  $B$ -mode polarization, Millimeter wave, TES bolometer

## 1 Introduction

### 1.1 Motivations for $B$ -mode studies

Since its discovery in 1964, the cosmic microwave background (CMB) has been one of the most important sources of cosmological information. Many observations have been performed since then, and observation technology has also greatly advanced (see review in [1] and references therein). A front line is the observation of  $B$ -mode polarization, which is a pattern characterized by odd-parity in spatial inversion.

A goal of  $B$ -mode polarization observation is to provide evidence of a nonzero tensor-to-scalar ratio,  $r$ . It is defined as the ratio of the amplitudes of the tensor and scalar perturbations in the early universe. Tensor perturbations are only caused by primordial gravitational waves that are generated by cosmic inflation [2, 3]. Therefore, a nonzero  $r$  would provide evidence of the inflation, and if discovered, the value of  $r$  would help to distinguish between inflation models. Another motivation for observing  $B$ -mode is to measure the sum of neutrino masses  $\Sigma_{i=1}^3 m_\nu^i$  [4, 5]. The  $B$ -mode anisotropies at small scales arise from  $E$ -mode by the effect of gravitational lensing, which are sensitive to  $\Sigma_{i=1}^3 m_\nu^i$ .

### 1.2 Concept of POLARBEAR and Simons Array experiments

The POLARBEAR (PB) experiment is designed to observe the CMB polarization and is mounted on the Huan Tran Telescope (HTT). With a primary mirror of 2.5 m effective diameter and with a continuously rotating half-wave plate (HWP) [6], PB achieved high sensitivity across a wide multipole range where both primordial gravitational waves and gravitational lensing  $B$ -modes are included. The original PB experiment began PB-1 observations in year 2012. Our results were published in papers [7–12].

The Simons Array (SA) is an upgrade of the PB experiment with three telescopes with newly designed receivers. Two additional telescopes of the same design<sup>1</sup> have been built next to the original HTT. The new receivers are called POLARBEAR-2A (PB-2A), POLARBEAR-2B (PB-2B), and POLARBEAR-2C (PB-2C), respectively by the order in which they are manufactured. The number of detectors per receiver is 7588: about six times more than that of PB-1. PB-2A and PB-2B are equipped with dichroic sensors to detect 90 GHz and 150 GHz bands. PB-2C also has dichroic sensors, but these are sensitive to frequency bands centered at 220 and 270 GHz to detect thermal dust radiation. Because of additional frequency bands, SA will be able to more reliably separate the CMB signal from those produced by foreground sources.

Science, the University of Tokyo · <sup>af</sup>Radio Astronomy Laboratory, University of California, Berkeley · <sup>ag</sup>Research Center for the Early Universe, School of Science, the University of Tokyo · <sup>ah</sup>Laboratoire de l'Accélérateur Linéaire · <sup>ai</sup>Department of Physics, Stanford University · <sup>aj</sup>Intel Corporation · <sup>ak</sup>National Astronomical Observatory of Japan, E-mail: daisuke.kaneko@ipmu.jp

<sup>1</sup> The Nicholas Simons Telescope (North), and The Paul Simons Telescope (South)

The expected sensitivities at SA are  $\sigma(r) = 0.006$  for  $r = 0.1$ , and  $\sigma(\sum_{i=1}^3 m_\nu^i) = 40$  meV for the sum of neutrino masses. Both values are in 68% C.L., after 3 years of observation with expected performance, foreground reduced, and degeneracy mitigated with future optical surveys such as DESI [13].

## 2 Design of POLARBEAR-2A

A cross-sectional image of the PB-2A receiver is described in Fig. 1. The receiver can be separated into two sections: an “optics tube” and a “backend”. CMB light enters the receiver through the window of the optics tube and finally focuses on the detector located at the backend.

### 2.1 Optical system

The HTT adopts a Gregorian-Dragone configuration [14] which can compensate for cross polarization made by each mirror. A receiver system is located around the Gregorian focus of the telescope. The POLARBEAR-2A receiver comprises a cryostat with three shells cooled by pulse tube refrigerators. The chambers inside are supported by insulating fiberglass laminate struts, and multilayer reflective insulators are installed to reduce thermal conduction. The outermost 300 K shell is also a vacuum chamber.

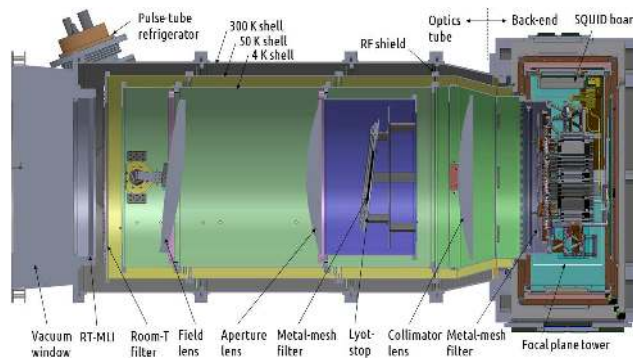


**Fig. 1** Cross-sectional image of POLARBEAR-2A receiver. The cryostat has 300 K, 50 K, and 4 K shells. Light enters the receiver from foamed polypropylene window (50 cm diameter, 20 cm thickness) at the left side.

The optics tube contains a re-focusing optical system that consists of three alumina lenses. Details of fundamental optical design are found elsewhere [15]. To reduce reflections caused by the high refractive index (3.10) of alumina, two types of anti-reflection coatings are applied. A two-layered epoxy resin [16] is used for each curved face, and a sprayed mullite and porous-polyimide sheet [17] is used for each flat face. Radio transparent multi-layered insulators (RT-MLIs [18]), an alumina filter and low-pass metal mesh filters are installed in the optical system to reduce the thermal load. The aperture (Lyot) stop is put inside the 4 K shell and tile-shaped epoxy based black body (KEK-black) [19] is mounted at its surface. The same black body absorber is applied to the inner surface of the 4 K shell.

## 2.2 Detector

Fig. 2 shows the PB-2A detectors assembled in the focal plane tower (FPT). A 3-stage He sorption refrigerator cools the FPT. Seven detector modules are attached to the stage of 0.3 K. Each detector module comprises a detector wafer inserted in an invar wafer holder, lenslets, and readout modules for multiplexing readout. PB-2A adopts transition edge sensor (TES) bolometer technology [20, 21]. The TES utilizes a very steep resistance change at superconducting transition. The TES of PB-2A is composed of an AlMn alloy and is operated with constant voltage bias.

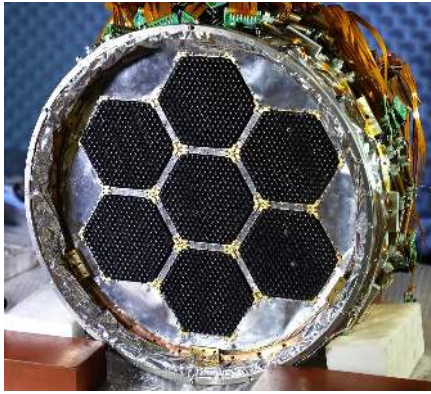


**Fig. 2** Assembled focal plane tower. Each with the seven hexagonal structure is a detector module, and the surface is covered with lenslets.

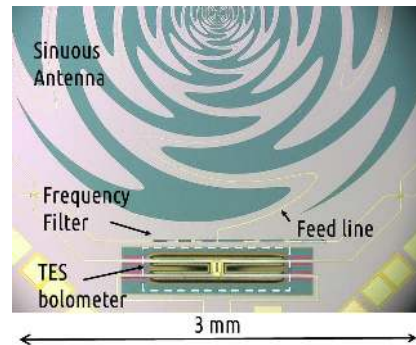


**Fig. 3** Microscopic image of sinuous antenna and detector which are processed on a silicon wafer. The TES is located at the center of dashed rectangle.

The incident photons are coupled to an antenna by a silicon lenslet. Fig. 3 provides a zoomed-in photograph of a sinuous antenna. It is sensitive to two orthogonal linear polarizations and provides uniform response over a wide frequency range. A load resistor coupled with the antenna and the TES are on an “island”, and heat from the load resistor transmits to the TES.

## 2.3 Readout system

A schematic of the TES readout is shown in Fig. 4 [22]. PB-2A uses Digital Frequency-Division Multiplexing (DfMux) of factor 40 to reduce the thermal loading from outer electronics, and the total number of cables. In the DfMux method, TESs are coupled with LC resonators of different resonant frequencies and bias voltages are supplied in corresponding mixed frequencies. The multiplexed TES currents travel over low-inductance thermally insulating cables where they are transduced into a voltage by a SQUID array operating at 4 K. Input signal generation, output digitization, and network communication are controlled with “ICE boards” [23], FPGA-based electronics, installed in telescope comoving crates. The sampling frequency is 152 Hz for all channels. Data stored at the front-end computer is transferred down-site to the foot of the mountain by a direct radio-link, subsequently, transferred to servers located in the United States and Japan using the Internet.

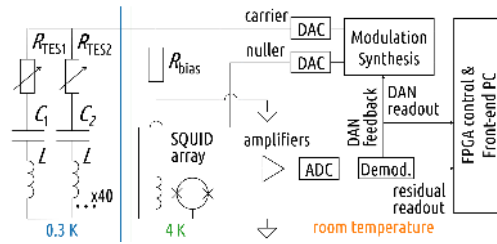


**Fig. 4** Schematic diagram of PB-2A readout. Stages of different temperatures are thermally insulated with NbTi cable (0.3 K - 4 K) and flexible wire harness (4 K - room Temp.).

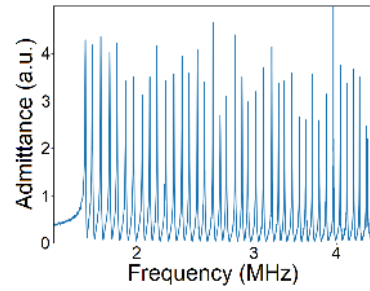


**Fig. 5** 40 different LC resonant peaks seen in laboratory test.

### 90 3 Validation of POLARBEAR-2A

#### 91 3.1 Laboratory testing

92 Integration tests of the PB-2A receiver were conducted with a fully installed detector array  
 93 and nearly all readout channels until the summer of 2018 at KEK, Japan. There are several  
 94 fundamental functionalities that had to be confirmed before shipping to the site: (a) evacua-  
 95 tion and cooling with refrigerators, (b) data acquisition tests with equivalent setup as the  
 96 site and (c) optical performance at cryogenic temperature.

97 The evacuation and cooling were tested successfully at nominal operation temperature  
 98 at 0.3 K for the detector stage. The typical hold time was 20 hours, which is long enough  
 99 to operate in a 24 hour cycle. As this value is under a condition with additional neutral  
 100 density filters for laboratory tests, the hold time should be a few hours longer without  
 101 the filters at the site. Second, data acquisition was checked with full-scale TES channels  
 102 under the same hardware configuration as that at the site [24]. Fig. 5 shows an example  
 103 of the DfMux readout, in which forty peaks corresponding to multiplexed channels are  
 104 clearly seen. The receiver noise was checked to ensure that the dominant noise was photon  
 105 noise but not readout noise ( $\sim 20 \text{ pA}/\sqrt{\text{Hz}}$  in normal conduction state). Third, the optical  
 106 transmission of optics tube was confirmed. The optical efficiency from the window to the  
 107 detector was measured with a liquid nitrogen vessel placed in front of the window. The  
 108 optical efficiency was found to be 23% / 21% for 90 / 150 GHz band, which is consistent  
 109 with the expectation.

110 The spectral performance of the detector was examined with a Fourier transform spec-  
 111 trometer [25]. Some TESs of both bands are measured. Measured band centers were 85.2 /  
 112 143.9 GHz, band widths were 18.3 / 22.1 GHz for 90 / 150 GHz band channels, which were  
 113 within the expected ranges. Spectroscopic tests for the entire detector array are planned at  
 114 the site. The detectors were upgraded after these measurements. Detection efficiency is ex-  
 115 pected to be improved with upgraded detectors that use silicon nitride as the dielectric [21].  
 116 Operation of calibrators like a stimulator (described later) are also tested in the laboratory.

#### 117 3.2 Site commissioning

118 In October 2018, the receiver was shipped to the Atacama Plateau. The assembly and in-  
 119 stallation onto the north telescope were completed in about one month and subsequently,  
 120 site commissioning began. The cryogenic system was soon stabilized to enable test oper-  
 121 ation, then readout tests were successively performed. The achieved noise in the best case  
 122 at the site is  $\sim 15 \text{ pA}/\sqrt{\text{Hz}}$  (in normal conduction state). The assembly and operation test  
 123 of the HWP have been finished.

1  
2  
3  
4  
5  
6  
7  
8  
9  
10  
11  
12  
13  
14  
15  
16  
17  
18  
19  
20  
21  
22  
23  
24  
25  
26  
27  
28  
29  
30  
31  
32  
33  
34  
35  
36  
37  
38  
39  
40  
41  
42  
43  
44  
45  
46  
47  
48  
49  
50  
51  
52  
53  
54  
55  
56  
57  
58  
59  
60  
61  
62  
63  
64  
65

124 *Stimulator* The stimulator is an artificial calibration source that uses black-body radiation  
125 from a ceramic heater (see Fig. 6). It is placed behind the secondary mirror, and signal  
126 is sent through a small hole in the mirror. In normal observations, stimulator data will  
127 be taken before and after each CMB scan and used for channel selection, relative gain  
128 calibration, and time-constant measurements. It is also used for many tests in deployment  
129 as a constant source. The signal was clearly seen with sufficient intensity by most ( $>90\%$ )  
130 of available detectors. Measured effective temperature is 45 / 70 mK for 90 / 150 GHz  
131 bands.

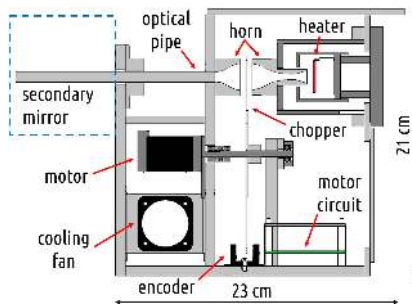


**Fig. 6** Design of the stimulator for PB-2A. A ceramic heater (700 deg C) is covered in total three layers of covers. The chopper modulates signal from 5 to 44 Hz.

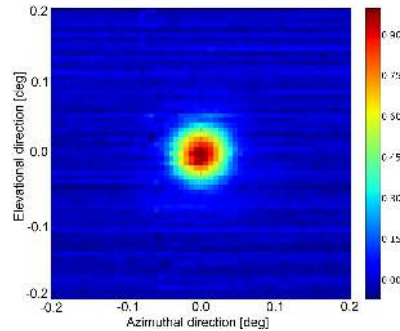


**Fig. 7** Observed image of Venus averaged over 150 GHz TESs in one detector module. This is a preliminary image before alignment of the receiver.

132 *Planet observations* Planet observations are useful for beam-shape characterization be-  
133 cause planets are effectively point-like sources. We achieved the first light with an obser-  
134 vation of Venus in January 2019. Fig. 7 is the first planet image which we observed with  
135 POLARBEAR-2A. Although the telescope had not yet been optimally aligned at this stage,  
136 data from several detectors during this scan showed circular images of Venus. Measured  
137 beam widths were 5.8 / 3.8 arcmin in FWHM for 90 / 150 GHz channels, while design  
138 values are 5.0 / 3.5 arcmin. More recently, other planets such as Jupiter and Saturn, have  
139 been observed as well. These planet images are being used for alignment of the telescope  
140 and absolute scale calibration.

#### 141 4 Conclusion

142 PB-2A, the first receiver for the Simons Array, is expected to have higher performance  
143 than the original PB-1, with about 6 times as many TES detectors as those of PB-1. Labo-  
144 ratory tests have finished and the PB-2A was deployed to the site in the Atacama Plateau.  
145 We achieved a successful operation of thousands of TESs and the first light with PB-2A  
146 was received in planet observations. The commissioning work continues to validate all the  
147 system to start CMB science observations.

148 **Acknowledgements** The Simons Array is supported by the Simons Foundation, the National Science  
149 Foundation (AST-1440338), the Moore Foundation, and the Heising-Simons Foundation. This work was  
150 supported by JSPS KAKENHI Grant Number JP26220709, JP15H05891, JP18H01240, JSPS Core-to-core  
151 Program, A.Advanced Research Networks., World Premier International Research Center Initiative (WPI),  
152 MEXT, Japan.

**References**

- 154 1. R. Durrel, *Classical and Quantum Gravity*, 32(12), (2015), DOI: 10.1088/0264-  
155 9381/32/12/124007
- 156 2. U. Seljak and M. Zaldarriaga, *Phys. Rev. Lett.* **78**, 2054 (1997)
- 157 3. M. Kamionkowski, A. Kosowsky, and A. Stebbins, *Phys. Rev. Lett.* **78**, 2058 (1997)
- 158 4. D. J. Eisenstein, W. Hu, and M. Tegmark, *Astrophys. J.*, **518**, 2, 23 (1998)
- 159 5. M. Kaplinghat, L. Knox, and Y.-S. Song, *Phys. Rev. Lett.* **91**, 241301 (2003)
- 160 6. C. A. Hill, et al, *Proc. SPIE*, 99142U (2016), DOI: 10.1117/12.2232280
- 161 7. P. A. R. Ade, et al. (POLARBEARCollaboration), *Phys. Rev. Lett.*, **112** 131302 (2014)
- 162 8. P. A. R. Ade, et al. (POLARBEARCollaboration), *Astrophys. J.*, **794**, 2, 171 (2014)
- 163 9. P. A. R. Ade, et al. (POLARBEARCollaboration), *Phys. Rev. Lett.*, **113**, 021301 (2014)
- 164 10. J. Errard, et al. (POLARBEARCollaboration), *Astrophys. J.*, **809**, 63 (2015)
- 165 11. P. A. R. Ade, et al. (POLARBEARCollaboration), *Phys. Rev. D*, **92**, 123509 (2015)
- 166 12. P. A. R. Ade, et al. (POLARBEARCollaboration), *Astrophys. J.*, **848**, 121 (2017)
- 167 13. A. Aghamousa, et al. (The DESI Collaboration), arXiv 1611.00036 (astro-ph.IM),  
168 (2016)
- 169 14. C. Dragone, *Bell Syst. Tech. J.*, **57**, 7 (1978)
- 170 15. F. T. Matsuda, Doctoral Thesis, University of California San Diego, (2017)
- 171 16. D. Rosen, et al. *Appl. Opt.*, **52**, 33, (2013), DOI: 10.1364/AO.52.008102
- 172 17. Y. Inoue, et al. *Appl. Opt.*, **55**, 34, (2016), DOI: 10.1364/AO.55.000D22
- 173 18. J. Choi, et al. *Rev. Sci. Instr.*, **84**, 114502, (2013) DOI: 10.1063/1.4827081
- 174 19. Y. Inoue, Doctoral Thesis, Graduate University for Advanced Studies (SOKENDAI),  
175 (2016)
- 176 20. K. D. Irwin and G. C. Hilton, *Cryogenic Particle Detection*, C. Enss (Ed.), Springer-  
177 Verlag, (2005)
- 178 21. B. Westbrook, et al. *J. Low Temp. Phys.*, **193**, 758, (2018), DOI: 10.1007/s10909-018-  
179 2059-0
- 180 22. K. Hattori, et al, *Nucl. Instr. Meth. A*, **732**, 299-302, (2013), DOI:  
181 10.1016/j.nima.2013.07.052
- 182 23. K. Bandura, et al, *J. Astron. Instr.* **05**, 1641005, (2017)
- 183 24. D. Barron et al., *Proc. SPIE*, 1070808, (2018), DOI: 10.1117/12.2311502
- 184 25. F. Matsuda, et al., *Rev. Sci. Instr.* **90**, 115115 (2019), DOI: 10.1063/1.5095160,  
185 arXiv:1904.02901 (astro-ph.IM)